A Novel Variable Refrigerant Flow (VRF) Heat Recovery System Model: Development and Validation

Rongpeng Zhang[1], Kaiyu Sun[1], Tianzhen Hong[1]*,
Yoshinori Yura[2], Ryohei Hinokuma[3]

[1] *Building Technology and Urban Systems Division, Lawrence Berkeley National Laboratory, Berkeley, CA 94720, USA*
[2] *Daikin Industries LTD, Nakazaki-Nishi, Kita-ku, Osaka, 530-8323, Japan*
[3] *Daikin US Corporation, New York, NY 10017, USA*

* Corresponding author: thong@lbl.gov, 1(510)486-7082

Abstract

As one of the latest emerging HVAC technologies, the Variable Refrigerant Flow (VRF) system with heat recovery (HR) configurations has obtained extensive attention from both the academia and industry. Compared with the conventional VRF systems with heat pump (HP) configurations, VRF-HR is capable of recovering heat from cooling zones to heating zones and providing simultaneous cooling and heating operations. This can further lead to substantial energy saving potential and more flexible zonal control. In this paper, a novel model is developed to simulate the energy performance of VRF-HR systems. It adheres to a more physics-based development with the ability to simulate the refrigerant loop performance and consider the dynamics of more operational parameters, which is essential for representing more advanced control logics. Another key feature of the model is the introduction of component-level curves for indoor units and outdoor units instead of overall performance curves for the entire system, and thus it requires much fewer user-specified performance curves as model inputs. The validation study shows good agreements between the simulated energy use from the new VRF-HR model and the laboratory measurement data across all operational modes at sub-hourly time steps. The model has been adopted in the official release of the EnergyPlus simulation program since Version 8.6, which enables more accurate and robust assessments of VRF-HR systems to support their applications in energy retrofit of existing buildings or design of zero-net-energy buildings.

Keywords:
Variable Refrigerant Flow; heat recovery; energy modeling; validation; building performance simulation; controls

1 Introduction

The building sector has become the largest consumer of primary energy in the world, exceeding both the industry and the transportation sectors. This leads to enormous fossil fuel consumption as well as severe environmental impacts [1,2]. It has been well recognized that it is crucial to improving the energy efficiency of building HVAC system which accounts for almost half of the total energy consumption in commercial buildings [3,4]. It is also believed that there will be a significant increase of HVAC installations globally with the growing demand for more comfortable built environment. Therefore, HVAC system performance has obtained extensive attention and numerous energy saving methods and technologies are developed to improve it [5,6].

As one of the emerging building technologies, Variable Refrigerant Flow (VRF) system has been widely adapted in Asia and Europe for decades and is obtaining a fast-growing market share in North America [7,8]. It is a multi-split air-conditioning system that is capable of varying the flow rate of refrigerant going to the indoor units of each zone independently and in tune with the diverse and dynamic space cooling or heating load, by making use of a number of advance control techniques including the variable speed fan, variable capacity compressor with inverter technology, and electronic expansion valve. It incorporates an air-source or water-source outdoor unit, multiple indoor units, refrigerant piping loop, distribution units, and the corresponding system and zone controllers [9,10].

The energy performance of VRF systems has been extensively studied via field or laboratory measurement or numerical analysis. In general, VRF can provide exceptional part-load efficiency and highly responsive cooling and heating performance by taking advantage of the variable speed compressor in the outdoor unit as well as the variable speed fan and electronic expansion valves (EEV) in the indoor unit [11]. The heat recovery system can achieve even higher energy efficiency by making use of waste heat. Many scholars evaluated the energy performance of VRF by comparing with various types of conventional HVAC systems. Aynur and Hwang *et al.* performed a simulation comparison of VRF and VAV in an existing building located in U.S. and concluded that an energy saving of 27–58% can be achieved [12]. Yu and Yan *et al.* investigated the VRF systems in five typical office buildings in China. It is found that the cooling energy can be reduced by up to 70% compared with typical VAV systems mainly because of the significantly fewer operating hours and the higher cooling setpoint of VRF resulting from different operation modes and control logics [13]. It is also found that VRF can save more than 20% energy consumption compared with fan-coil plus fresh air system and 15-42% compared to rooftop variable air volume systems [13–15]. It should be noted, however, the energy performance of VRF is affected by the building use and system configurations, and therefore its saving potential may vary for different cases. For example, in an experimental study on the ground source heat pump (GSHP) system

and VRF system at ASHRAE Headquarter [16–18], it is found that GSHP presents higher energy efficiency. Similar findings are also obtained in a simulation study conducted by Hong and Liu [19] in a small office building.

In addition to the energy-saving performance, VRF presents a number of other significant advantages in terms of control capability, design flexibility and ease of installation and maintenance. More specifically: (1) VRF system allows the installation of more than sixty indoor units supported by one single or multiple outdoor units. The extraordinary zonal control capability makes VRF a satisfying candidate for the situations where there is an advantage to deliver individualized comfort conditioning. It is also widely chosen for nursing homes and hospital buildings where there is a need to avoid zone-to-zone air mixing to reduce the airborne transmission, (2) VRF system presents high layout design flexibility and modular installation advantages, which makes it particularly suitable for retrofitting historical buildings without disturbing the structure, and (3) VRF systems have several other advantages including low noise levels and space-saving. This brings VRF systems extra credits for the buildings where quiet conversations are paramount or strict noise regulations may apply, such as classrooms, schools, universities, healthcare facilities, and libraries [6,7,13,20,21].

Manufacturers and scholars have also been making continuous efforts to develop new advanced features to improve VRF performance. Some studies focus on the introduction of enhanced component design or integrated operation with other systems. For example, Aynur *et al.* presented a new design of VRF with a self-regenerating heat pump desiccant unit, and explored the integrated performance in dehumidification operations by performing field measurements [22]. Li and Wu investigated the operational characteristics of a VRF system with water-cooled condensers [23]. Zhu and Jin introduced an optimal control logic for an integrated VRF and VAV system and obtained remarkable performance improvement [24]. Some other studies focus on the development and implementation of enhanced control logics. One successful example is the variable refrigerant temperature (VRT) technique, which can automatically manipulate refrigerant temperature at various operational conditions in addition to the modulation of the refrigerant flow rate. It evaluates the load conditions of all the spaces served by the system and determines the dynamic optimized refrigerant temperature levels for better operational performance. This technique has been successfully applied in the latest VRF products on the market [20,25,26].

VRF system can be generally divided into two types in terms of air-conditioning functionality: heat pump (VRF-HP) and heat recovery (VRF-HR). VRF-HP is able to supply either heating or cooling to different spaces but cannot provide heating and cooling simultaneously. By contrast, VRF-HR can recover the heat from the indoor units at cooling zones to serve the zones that are currently in the heating mode,

and thus is able to achieve simultaneous heating and cooling functions. Because it can reuse the heat extracted locally from the indoor units, the capacity of a VRF-HR outdoor unit can be theoretically reduced compared with that of a VRF-HP system. The heat recovery mode is normally more prominent in shoulder seasons or applications with a wide variety of zone diversity (by orientation, use type and occupancy), such as medium- to large-sized commercial buildings with a substantial core area of a data center or server rooms [9,27,26].

Performance-based empirical VRF models have been developed for both the HP and HR systems and implemented in a variety of building simulation programs [7,10,28]. These equation-fitting models are developed based on a number of system-level curves which can describe the overall system's operational behavior. For instance, there are specific curves to parameterize the variation of system capacity and power as a function of operating conditions, including the compressor part-load ratio, combination ratio, and indoor/outdoor air conditions, the [9,29]. The existing empirical models can usually present satisfying performance to evaluate the traditional VRF systems under normal operational conditions. When it comes to the advanced VRF systems with more complicated control logics, however, these models often have insufficient capability for accurate system performance estimation mainly because of limited access to the system operational parameters. For example, to calculate the thermal loss in the main refrigerant piping network, the empirical VRF model could not access the dynamic refrigerant operational conditions, therefore it roughly estimates the heat loss with a constant correction factor without capturing the heat loss variations under various operational conditions. This constraint further limits the model's capability to simulate the variable evaporating and condensing temperature control logics and may considerably affect the simulation accuracy under certain scenarios. Another example is the modeling of advanced VRF control algorithm at low load conditions, in which the adjustment of superheating and subcooling degrees is essential. The current empirical VRF model, however, cannot access the superheating and subcooling parameters and therefore is not capable of addressing such control algorithm.

With more adoption of VRF technologies in designing new or retrofitting existing buildings to reach the zero-net-energy goal, it is critical to have an accurate tool to assess the performance of VRF systems. The paper aims to develop a more physics-based model to simulate the energy performance of VRF-HR systems. This is a continuation of our previous study on the development of a physics-based VRF-HP model [20] which was implemented in EnergyPlus version 8.4 [9]. The model categorizes the operations of the VRF-HR system into six modes based on the indoor cooling/heating requirements and the outdoor unit operational states, and uses novel algorithms to capture the control logic and heat recovery between indoor units. The work presented in this paper introduces the development, implementation and validation

of the new model.

2 VRF-HR System Operation

2.1 VRF-HR System Configurations

VRF-HR system is more complicated than VRF-HP in terms of the configurations and controls of the system. VRF-HR system can be further divided into 3-pipe type and 2-pipe type based on the design of the component and piping connections. The 3-pipe system is the dominant type in the existing VRF-HR market.

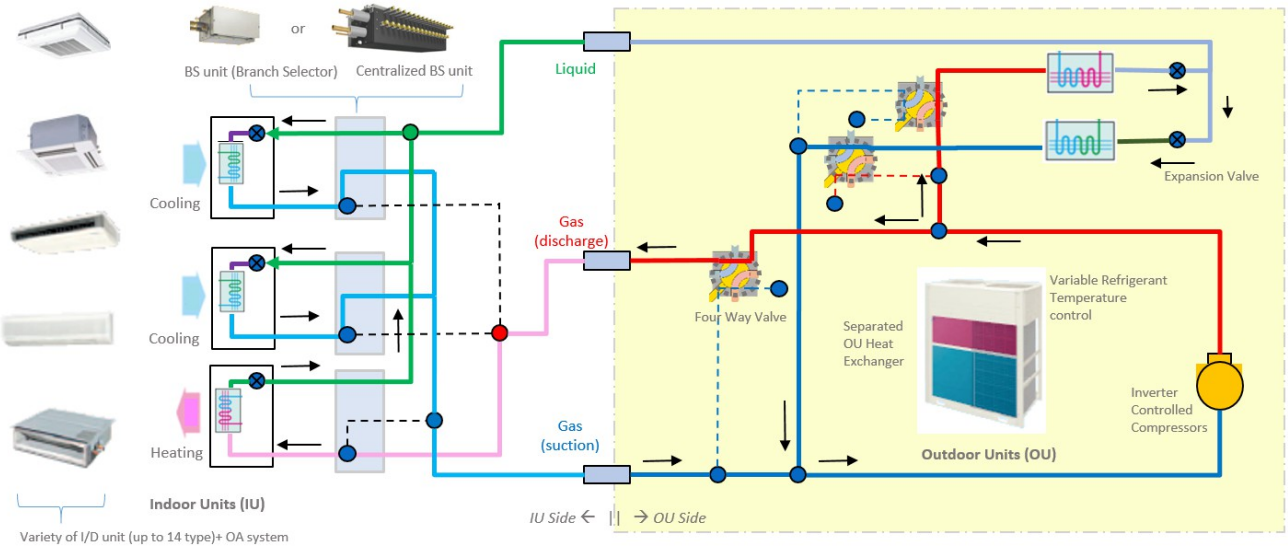

Figure 1 Schematic chart of a 3-pipe VRF-HR system

Figure 1 shows the component and piping connections of a typical 3-pipe VRF-HR system. As can be seen, the VRF-HR system has three dedicated refrigerant pipes for suction gas, liquid and discharge gas, respectively. To enable simultaneous cooling and heating, complex refrigerant management loop, and more system components are implemented, including one additional heat exchanger in the outdoor unit and multiple Branch Selector (BS) Units. The two heat exchangers in the outdoor unit can work at different evaporator/condenser combinations to enable specific operational modes for diverse and changing indoor heating/cooling load requirements. Some manufacturers may have outdoor units with an additional heat exchanger for the circuit that realizes the refrigerant cooled electrical box. In order to automatically switch the indoor operational mode from cooling to heating or vice versa, the system implements a number of Four-Way Directional Valves (FWV) and BS units, which enable the system to provide separate refrigerant piping connections for different operational modes. This leads to varying

refrigerant flow directions and different control logics and therefore requires specific algorithms for different operational modes.

2.2 Definition of Six Operation Modes

Depending on the indoor cooling/heating requirements and the outdoor unit operational states, the operations of the VRF-HR system can be categorized into six modes:

- Mode 1: Cooling load only. No heating load. Both outdoor unit heat exchangers operate as condensers.
- Mode 2: Simultaneous heating and cooling. The sum of the zone cooling loads and compressor heat is much larger than the sum of the zone heating loads. Both outdoor unit heat exchangers operate as condensers.
- Mode 3: Simultaneous heating and cooling. The sum of the zone cooling loads and compressor heat is slightly larger than the sum of the zone heating loads. One outdoor unit heat exchanger operates as a condenser while the other as an evaporator.
- Mode 4: Simultaneous heating and cooling. The sum of the zone cooling loads and compressor heat is slightly smaller than the sum of the zone heating loads. One outdoor unit heat exchanger operates as a condenser while the other as an evaporator.
- Mode 5: Simultaneous heating and cooling. The sum of the zone cooling loads and compressor heat is much smaller than the sum of the zone heating loads. Both outdoor unit heat exchangers operate as evaporators.
- Mode 6: Heating load only. No cooling load. Both outdoor unit heat exchangers operate as evaporators.

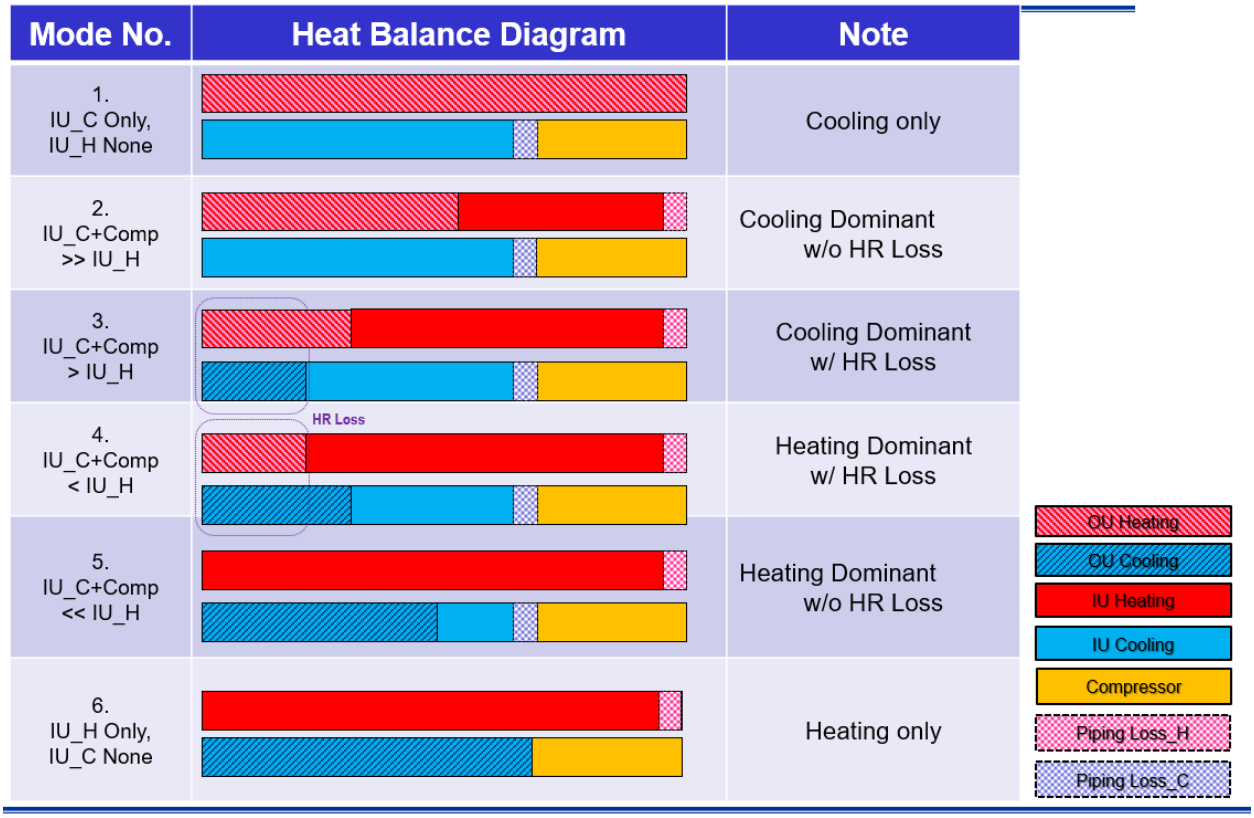

Figure 2 VRF-HR Operational Modes: System-level Heat Balance Diagram

The system-level heat balance diagram for all the six operation modes is shown in Figure 2. One concept to note in the diagram is the heat recovery loss (HR loss), which is an inherent characteristic of the VRF-HR systems when operating in Mode 3 and Mode 4 where the outdoor unit evaporator and condenser run simultaneously. In these two modes, the following two items are at similar levels: (a) the sum of IU heating loads and IU condenser side piping loss, and (b) the sum of IU cooling loads, IU evaporator side piping loss and heat released by the compressor. Taking Mode 3 for example, item (b) is higher than item (a). Therefore the system requires the operation of the outdoor unit condenser to release the extra heat to ensure the system-level heat balance. However, the extra heat is at a relatively low level, which means the system needs to release more heat than required via an outdoor unit condenser, and meanwhile, runs the outdoor unit evaporator to ensure the heat balance as well as system reliability. This leads to the presence of HR loss.

2.3 Piping Connection and Refrigerant Operation at Different Modes

With the help of FWV and BS units, every operation mode has particular refrigerant piping connections to achieve different refrigerant flow directions, as shown in Figure 3. This results in different refrigerant operations and piping loss situations, as shown in the Pressure-Enthalpy Diagrams in Figure 4.

Taking Mode 3 for instance, the system utilizes one outdoor unit heat exchanger as an evaporator and the other as a condenser. The superheated refrigerant coming out of the compressor is separated into two flows. One flow passes through the outdoor unit condenser within which the refrigerant is condensed and subcooled (segment 2-4'), while the other flow passes through the IU condenser to satisfy the indoor heating requirements (segment 3-4). Note that before entering the IU condenser, the second flow of the refrigerant flow passes through the main discharge gas pipe connecting the indoor and outdoor units, where the refrigerant pressure drop and heat loss occurs. This leads to extra heating load and a lower condensing temperature level at the IU condenser than that at the outdoor unit condenser. The two parts of refrigerant leaving condensers are then expanded through expansion valves following segment 4"-5/5' and pass through the IU evaporator (segment 5-6) and outdoor unit evaporator (segment 5'-1'). Similarly to the refrigerant passing through the main discharge gas pipe, the refrigerant leaving IU evaporators passes through the main suction gas pipe where the refrigerant pressure drop and heat loss occurs (segment 6-1"). This leads to extra cooling load and a higher evaporating temperature level at IU evaporator than that at outdoor unit evaporator. Finally, the refrigerant flow leaving the outdoor unit evaporator and that leaving the main discharge gas pipe are combined (segment 1'/1"-1) and enter the compressors for the next cycle. In this regard, the system provides simultaneous heating and cooling to the indoor environment.

A number of operational parameters are controlled to ensure system heat balance and stable operation, including evaporating temperature levels, condensing temperature levels, superheating and sub-cooling degrees, and the refrigerant flow rates at various components. The operational control logics for various modes are different and therefore particular algorithm needs to be designed for different operation modes in the new VRF-HR system model. More details of the control logics are described below in Section 3.

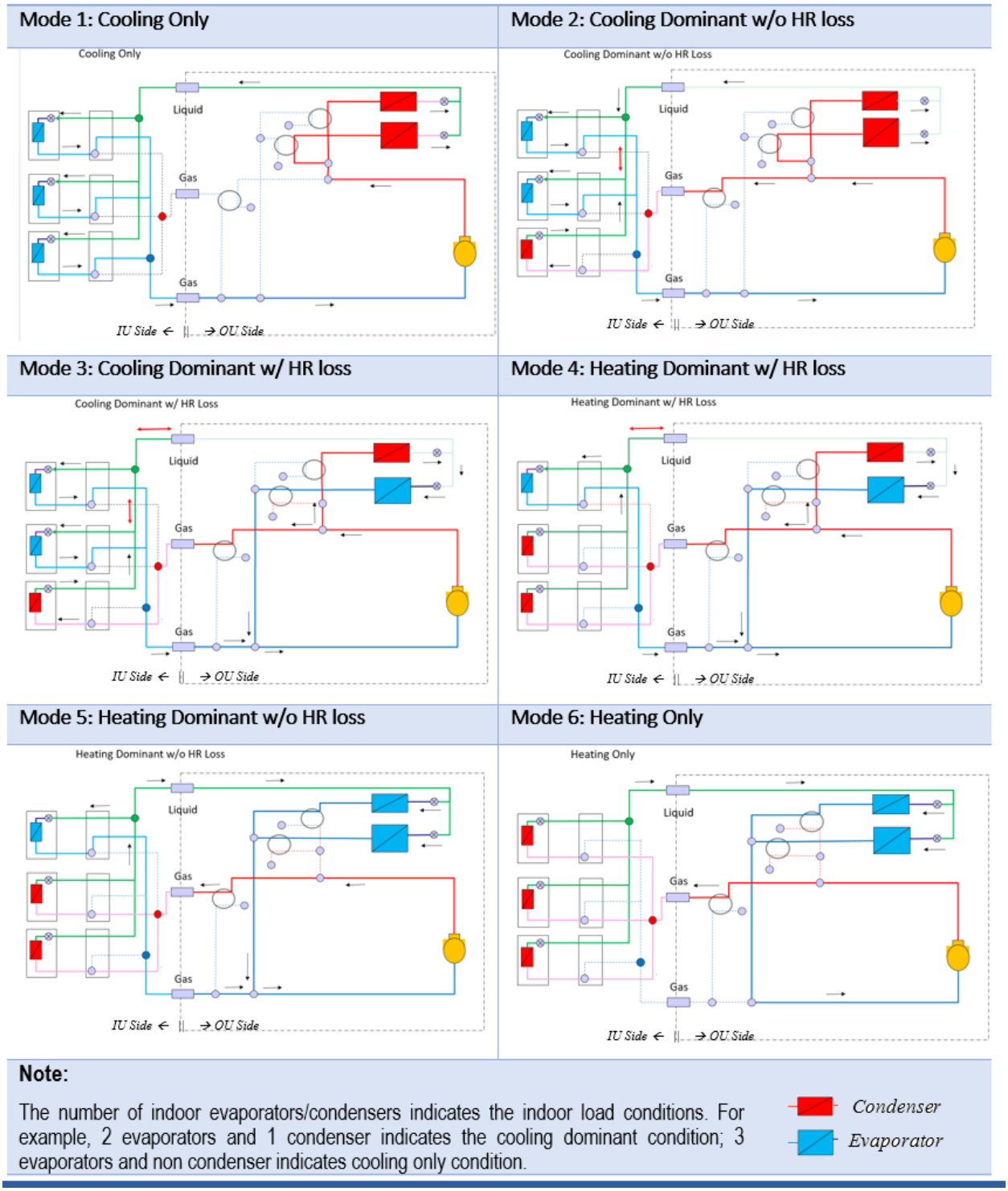

Figure 3 Piping diagrams for the six VRF-HR operation modes

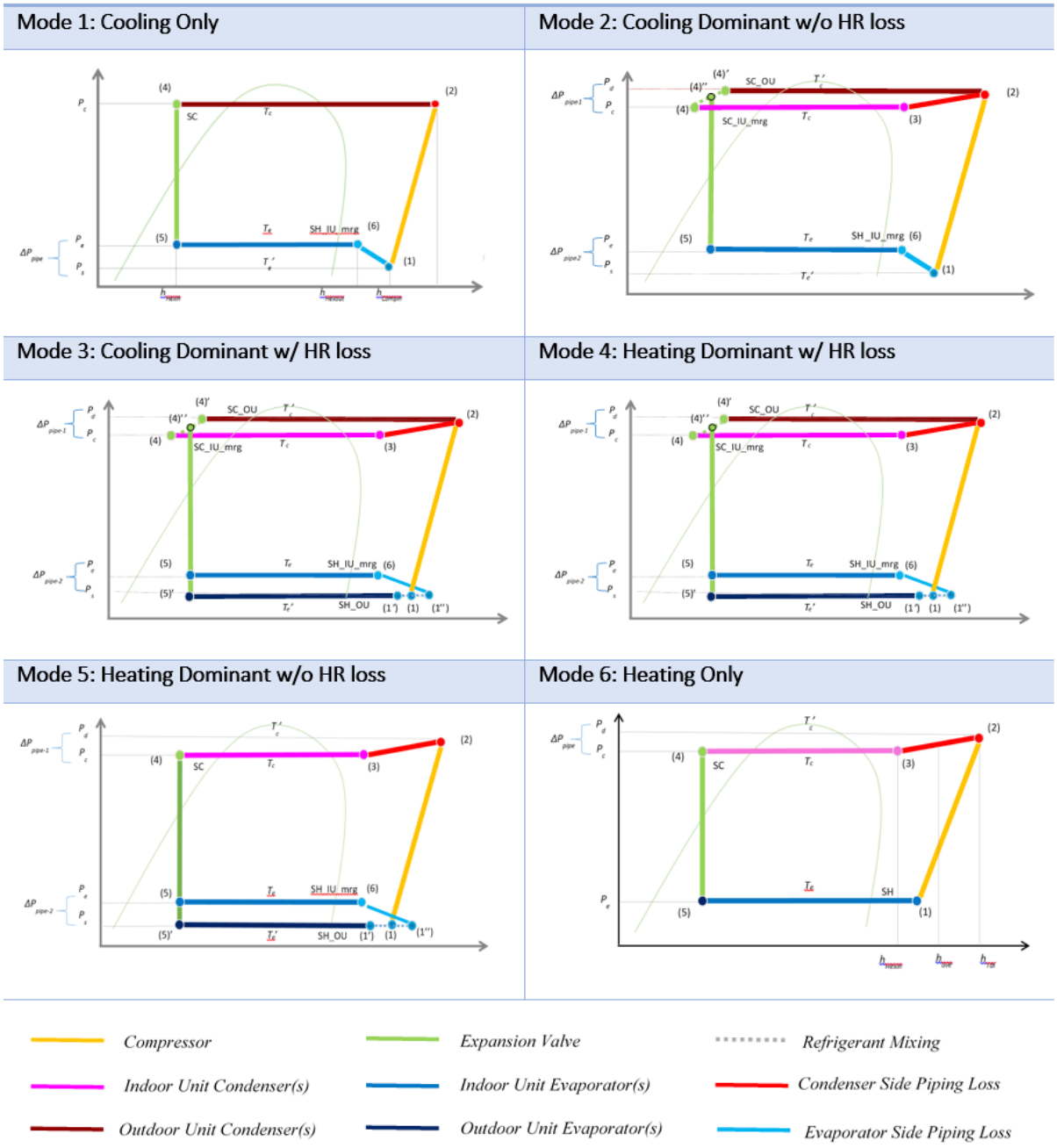

Figure 4 Illustration of the six VRF-HR operation modes on the Pressure-Enthalpy diagrams

3 Development of the New VRF-HR System Model

3.1 Key features of the new VRF-HR system model

To overcome the limitations of the system-curve-based empirical VRF-HR model, the new VRF-HR model implements a more physics-based development specifically in the following areas:

- Use component-level performance curves for key components of the indoor units and outdoor units, instead of the overall system-level curves, including [9]:
  1) Evaporating temperature as a function of superheating degrees
  2) Condensing temperature as a function of subcooling degrees
  3) Evaporative capacity as a function of evaporating and condensing temperatures and compressor load index
  4) Compressor power as a function of evaporating and condensing temperatures and compressor load index

  This allows the analysis of the component level performance and the cooperation between key components, enabling more flexibility for the models to address complex control logics.
- Use the physical model of the refrigerant piping loop. The new VRF model can calculate the refrigerant operational thermodynamic conditions based on the refrigerant type and its thermal properties specified by the user/modeler. It is also capable of addressing the refrigerant flow direction change at different operational modes. This allows the model to access the refrigerant-side system operational parameters (including refrigerant temperature, enthalpy, pressure, and flow rate) which are essential to model advanced refrigerant-side control logics. This further enables the physics-based calculation of thermal loss and pressure drop in the main refrigerant piping network which is a key step in the overall model development. More details on the piping loss calculations can be found in [20].

Note that the new VRF model implements component-level curves for the component performance estimation, therefore, it is more physics-based than the existing empirical VRF model, but it is not completely physics-based. Because of the complexity of the VRF-HR system, it is challenging or impossible for the user to collect all the detailed information (e.g., heat exchanger geometries and fin arrangement) to describe the system for thorough physics-based modeling.

The above features can offer the new model several considerable advantages in terms of modeling capability and usability. More specifically:

- Allowing the representation of the complex control logics, e.g., the adjustment of superheating degrees at the minimum compressor speed, and the variable condensing and evaporating

temperature control.

- Improving the usability of the model by significantly reducing the number of user specified performance curves as model inputs.
- Allowing the modeling of a single outdoor unit with multiple compressors or multiple OUs.
- Allowing the implementation of various control logics for different VRF-HR operational modes.
- Improving the simulation accuracy especially during partial load operations.
- Allowing more accurate estimation of HR loss, a critical characteristic parameter in the VRF-HR operations.
- Allowing further modifications of operational parameters (e.g., evaporating temperature and superheating degrees) during low load conditions.

In summary, these new features of the VRF-HR system model contribute to a new body of knowledge about modeling VRF-HR systems in buildings.

3.2 Summary of the algorithm at various modes

The holistic logics of the new VRF-HR model are illustrated in Figure to Figure , showing the key simulation steps for different operation modes. In general, the effective evaporating temperature and/or condensing temperature for the indoor units is first determined based on the load requirements and indoor unit configurations. Then the pressure and heat losses through the main pipe are calculated at the given operation conditions. After that, the effective condensing temperature and/or evaporating temperature of the outdoor unit are calculated taking into account the piping loss. With the above calculations, the compressor speed can be determined using the performance curves describing the evaporative capacity of the system at specific condensing/evaporating temperature combinations at various compressor speeds. Finally, the compressor power at that speed is calculated, and the total electric power consumption by the outdoor unit is obtained. Note that particular control logics are designed for various operation modes, and therefore lead to different refrigerant temperature adjustments. Also note that a number of calculation steps are coupled together, for instance, the piping loss calculation and the system performance calculation. More specifically, the piping loss changes the operating conditions of the system in certain specific conditions, which may lead to a different control strategy and thus affect the amount of piping loss. This makes it difficult to obtain an analytical solution for a number of operational parameters (e.g., enthalpy of refrigerant entering the indoor unit), and therefore numerical iterations are employed to address this problem.

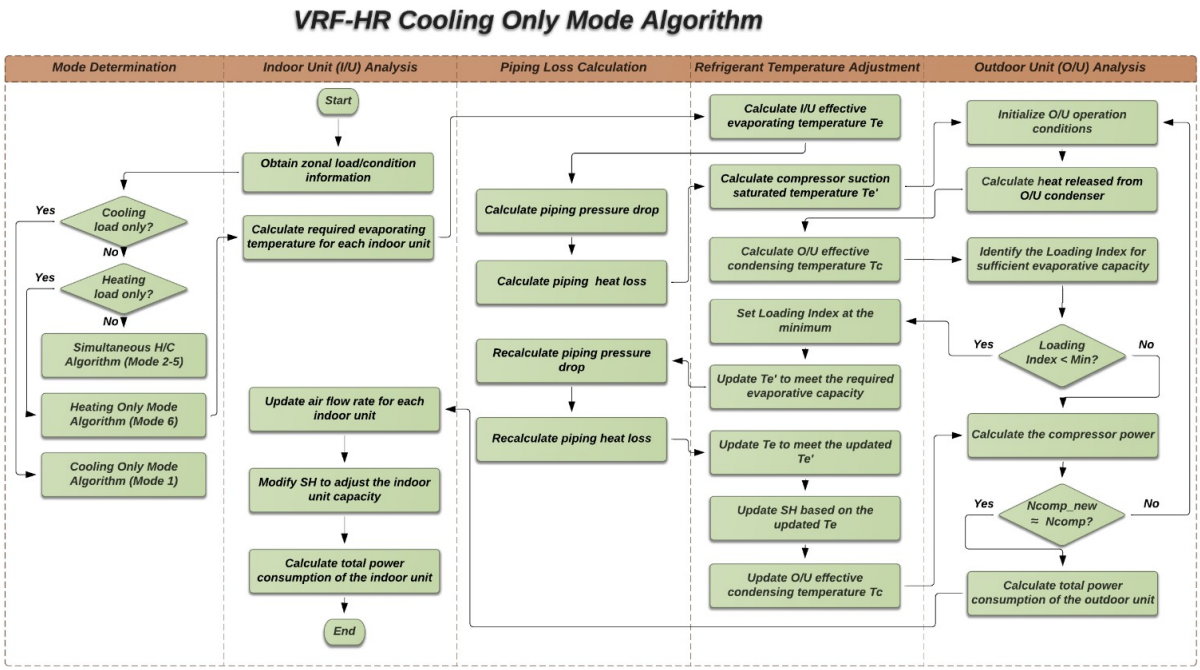

Figure 5 Schematic chart of the new VRF-HR model algorithm: Cooling Only Mode

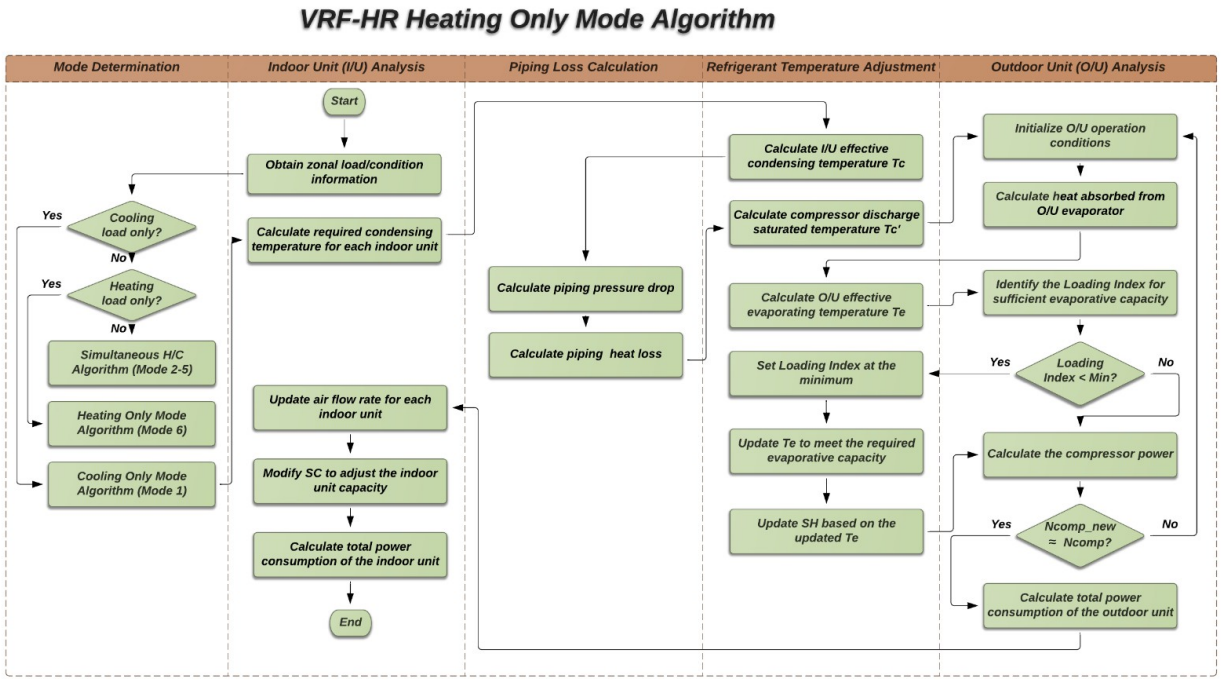

Figure 6 Schematic chart of the new VRF-HR model algorithm: Heating Only Mode

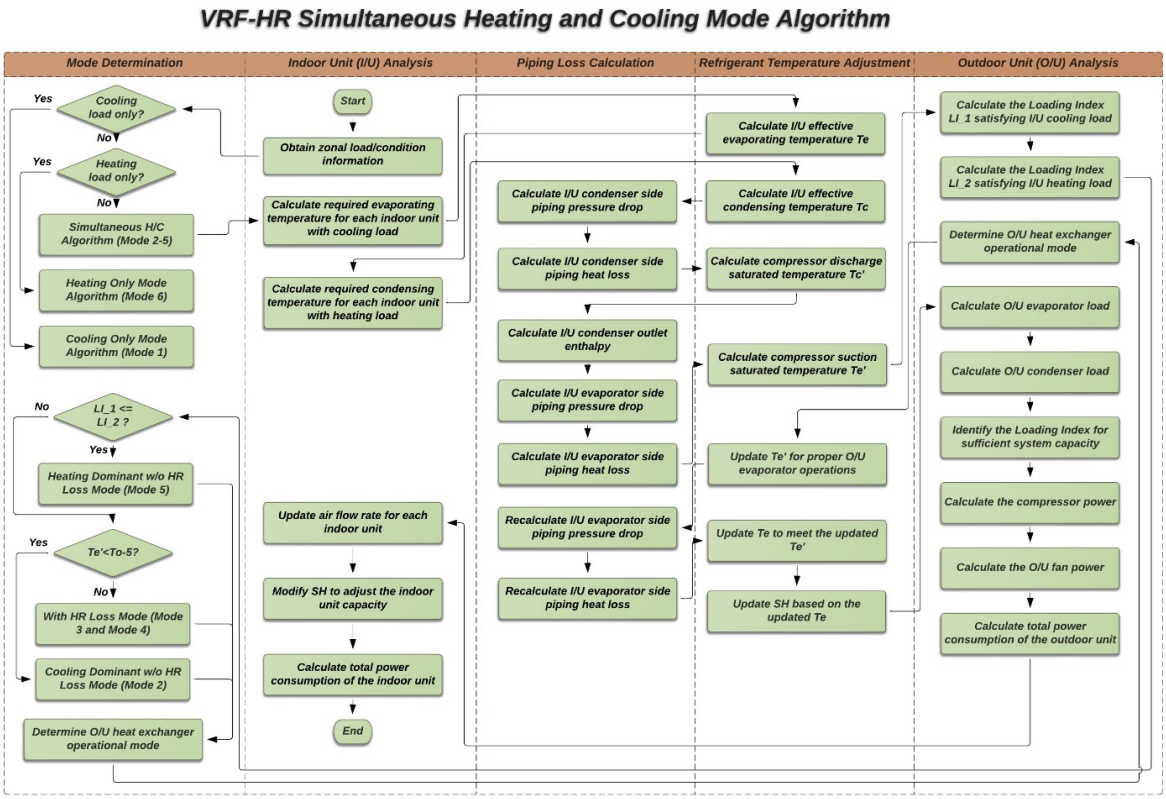

Figure 7 Schematic chart of the new VRF-HR model algorithm: Simultaneous Heating and Cooling Mode

The algorithm of the VRF-HR Cooling Only Mode (Figure 5) and the Heating Only Mode (Figure) are the same as those in the VRF-HP Cooling Mode and Heating Mode, respectively. Detailed calculation procedures for these two modes can be found in [20]. The calculation procedures for the VRF-HR Simultaneous Heating and Cooling Modes are summarized in Appendix A.

4 Model Implementation in EnergyPlus

As a continuation of the new VRF-HP system model implemented in EnergyPlus V8.4, the newly developed VRF-HR system model is implemented and validated in EnergyPlus and officially released in V8.6. EnergyPlus is a whole building performance simulation program developed under the lead of United States Department of Energy. It is capable of handling high-order building energy models containing the detailed information about the functional and physical characteristics of the buildings, and to perform co-simulation of a large number of subroutines to obtain more accurate estimations of the whole building performance, including cooling, heating, ventilation, lighting, water use, renewable energy generation and other energy flows. It is recognized as the flagship tool in the building simulation area and has been widely adopted by both the academia and industry to support more sustainable and energy-

efficient building design, retrofitting, and operation [9,30].

EnergyPlus implements an object structure to summarize the model input information on the building and system. In the new VRF-HR model, several specific objects are designed to describe the system configurations. Figure shows the organization of these objects to form the whole system model. The object describing the outdoor unit is the key part. It includes the information on the VRF specifications, such as refrigerant type, pipe size, component power and capacity. It also specifies the system operation and control, such as super-heating, sub-cooling, refrigerant temperature control, defrost strategy. This object connects to a zone terminal unit list object, containing multiple terminal unit objects which correspond to the indoor parts of the VRF system. The terminal unit object further refers to the objects of the indoor unit components, including the cooling coil, heating coil, mixer and fan. An example of IDF codes for the modeling of a typical VRF-HR system can be found in Appendix B.

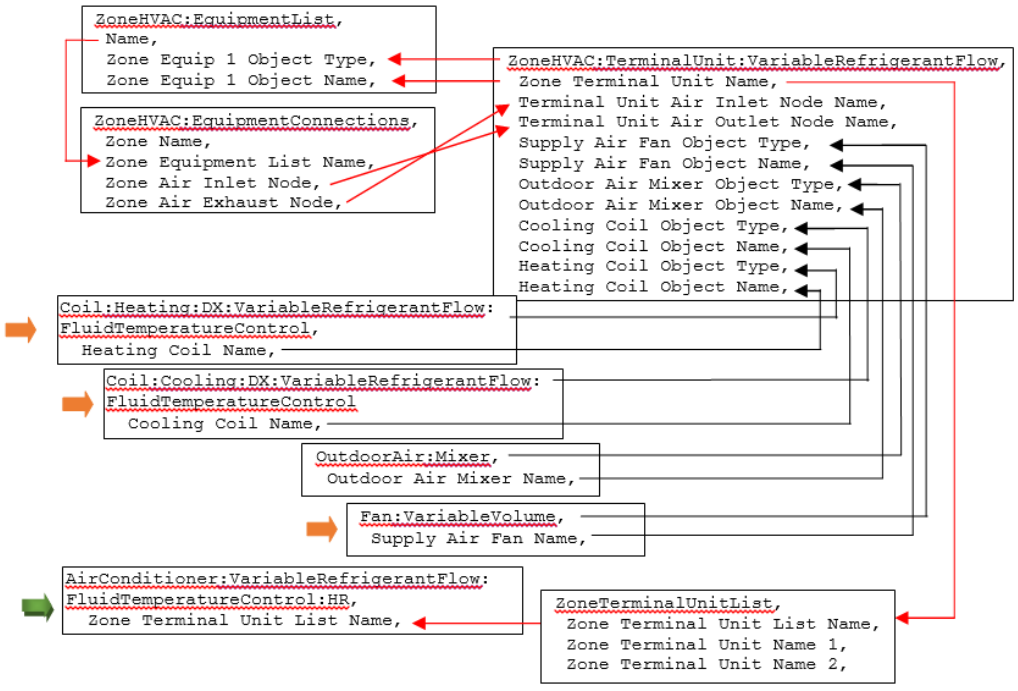

Figure 8 Object design and connection for the VRF-HR model in EnergyPlus (adapted from [9]*)*

5 Model Validation with Measurement Data

5.1 Laboratory Testbed Configuration

The model is validated with laboratory measurement data on a typical 3-pipe VRF-HR Multi-Split System. As indicated in Figure 99, the measurement platform includes one testbed acting as the outdoor unit and two testbeds acting as the indoor units. The outdoor unit is installed in the outdoor testbed with an embedded extra AC unit controlling the testbed temperature to represent various outdoor conditions.

The outdoor unit employs inverter controlled compressors which can vary the compressor operation mode for a variety of operational conditions. Each indoor testbed has the capability to generate the constant cooling/heating load by the embedded AC unit. Five terminal units are installed in the indoor testbed to create numerous heating/cooling combinations. The terminals supply conditioned air to the zone via a chamber where airflow rate is measured.

Sensors and meters are instrumented on both the air loop and refrigerant loop in the testbeds to perform dynamic measurement on the environmental conditions as well as the system operations. It aims to obtain comprehensive information on the system operational behavior. Some operational parameters can be directly measured in the test, such as the compressor speed and power consumption. Other operational parameters can be indirectly calculated using the direct measurement data. For example, the outdoor unit operation mode can be determined by identifying the role of heat exchangers, i.e., functioning as a condenser or an evaporator. This can be achieved by analyzing the heat exchanger capacity which is calculated based on the measured air side temperature, relative humidity, and airflow rate.

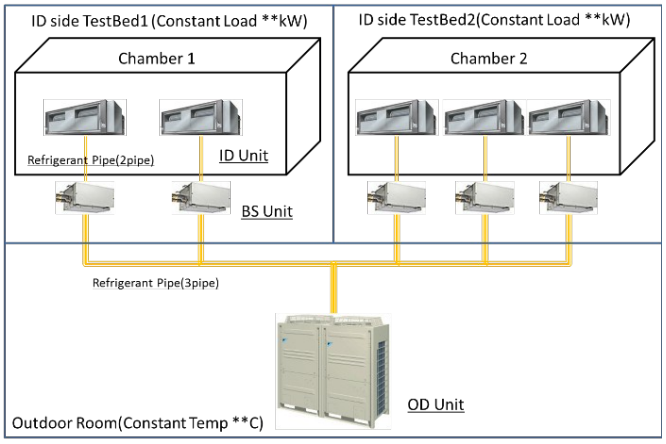

Figure 9 Schematic layout of the VRF-HR experiment testbeds

5.2 Measurement Condition Design

Comprehensive measurement data was collected for 15 static condition cases, as summarized in Figure 10. The indoor unit cooling and heating capacities are modulated to represent various indoor load requirements, and the outdoor air temperature level is modified to represent various outdoor operation conditions. The part-load ratio for simultaneous heating and cooling operations range from 5% to 45%, and the outdoor air temperature ranges from 37 to 63^{o}F (2.78 to 17.22^{o}C) which is the dominant outdoor temperature in simultaneous heating and cooling operation.

As aforementioned, there are six operation modes for the VRF-HR system: Mode 1 (Cooling only), Mode 2 (Cooling dominant without HR loss), Mode 3&4 (Simultaneous Cooling and Heating with HR

loss), Mode 5 (Heating dominant without HR loss), and Mode 6 (Heating only). The experiment conditions cover all the operational modes except for Mode 2 which presents relatively infrequent occurrence in actual system operations. As the operating status of the VRF-HR system is not constant throughout the whole testing period, a period of steady operation is selected from each experiment condition. It is noted that the operation mode is not only related to the simultaneous heating and cooling load but also the hysteresis of the operation mode, so it varies in the real operation even when the given load and temperature conditions are the same. The length of the periods could vary from a couple of minutes to half an hour with a measurement time interval of 10 seconds.

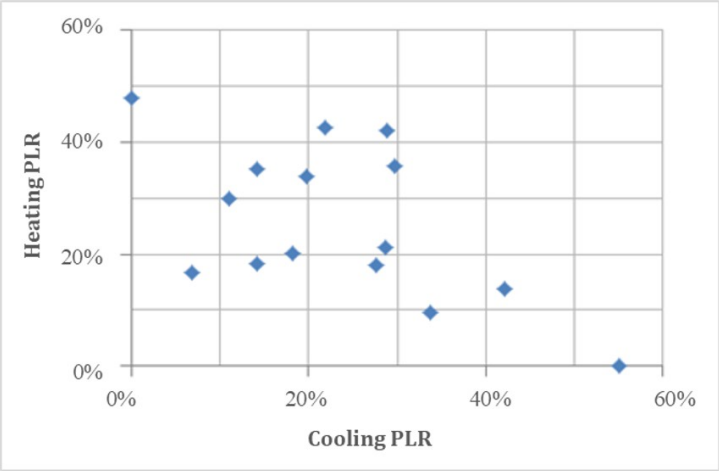

Figure 10 The experiment conditions of the VRF-HR system performance tests

5.3 Validation Procedure

To validate the VRF-HR algorithms, an EnergyPlus energy model with two zones is developed to represent the two testbeds with indoor units. The environmental conditions in the testbed with the outdoor unit are provided with a customized weather file. The sensible and latent loads in each indoor unit are calculated using the measurement data, and then input as the zone loads using the schedule object and equipment object. The model is then simulated using the new VRF-HR model in EnergyPlus and compared with the measured data to evaluate the accuracy of the algorithms.

Calibration criteria from ASHRAE Guideline 14 [31] are adopted for algorithm validation. When monthly data is compared, the model is considered calibrated if the absolute value of NMBE is less than 5% and CVRMSE is less than 15%. When hourly data is compared, the criteria of NMBE and CVRMSE are 10% and 30%, respectively.

The measured data were aggregated to the time interval of one minute in the validation, which is the minimum allowable simulation time step in EnergyPlus. Since sub-hourly data was used for comparison,

it is reasonable and rigorous to use the calibration criteria of hourly data for validation in this study.

5.4 Results and Discussions

The major target of the model is to determine the system operation mode at the given conditions and to estimate the system power consumption. Therefore, the comparison between the measured/simulated operation mode and compressor performance is conducted.

Validation results show that the new VRF-HR model can correctly determine the operation mode for all the test cases, which is essential for accurately estimating the compressor performance. Figure 11 depicts the comparison between the simulated and measured compressor speed, and Figure 32 illustrates the comparison of compressor power which is dependent on the compressor speed and refrigerant temperature levels. Figure 4 depicts the comparison of the total power consumption. It can be observed that the simulated compressor speed and power using the new VRF-HR model can present a satisfactory match with the measured data across all the operation modes at sub-hourly levels.

Note that the simultaneous heating and cooling modes generally show larger discrepancies than the heating or cooling only modes. This is mainly caused by the more complicated refrigerant piping network in the simultaneous heating and cooling modes, as can be observed in Figure 5. More specifically, Modes 1 and 6 only have the evaporator or condenser side piping loss, while Modes 2-5 have both. Additionally, the operations in Modes 2-5 have more refrigerant mixing processes, i.e., the subcooled refrigerant mixing and the superheated refrigerant mixing, which introduce modeling challenges for the simultaneous heating and cooling modes.

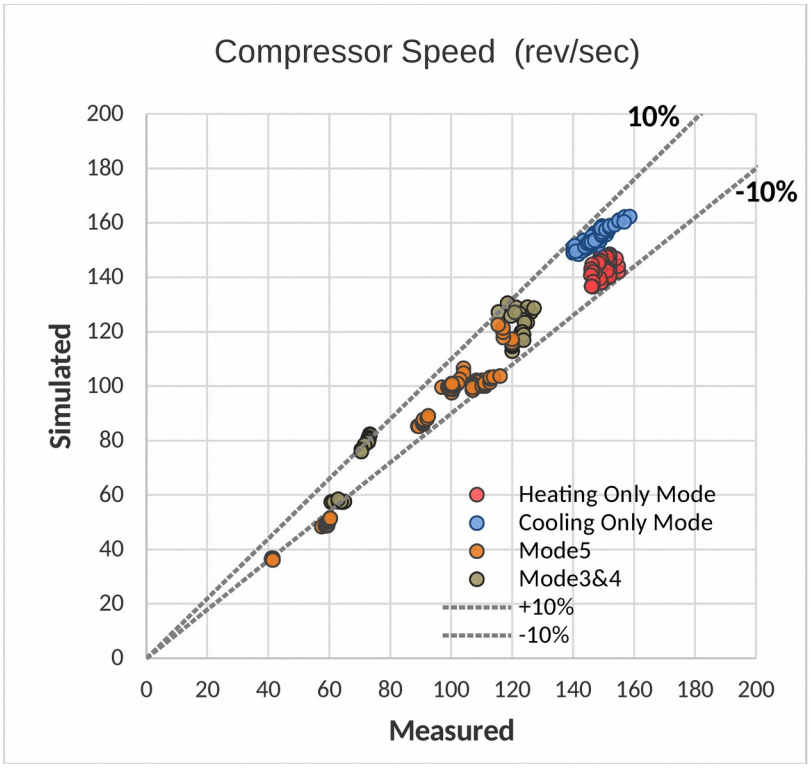

Figure 11 Comparison between the simulated and measured compressor speed

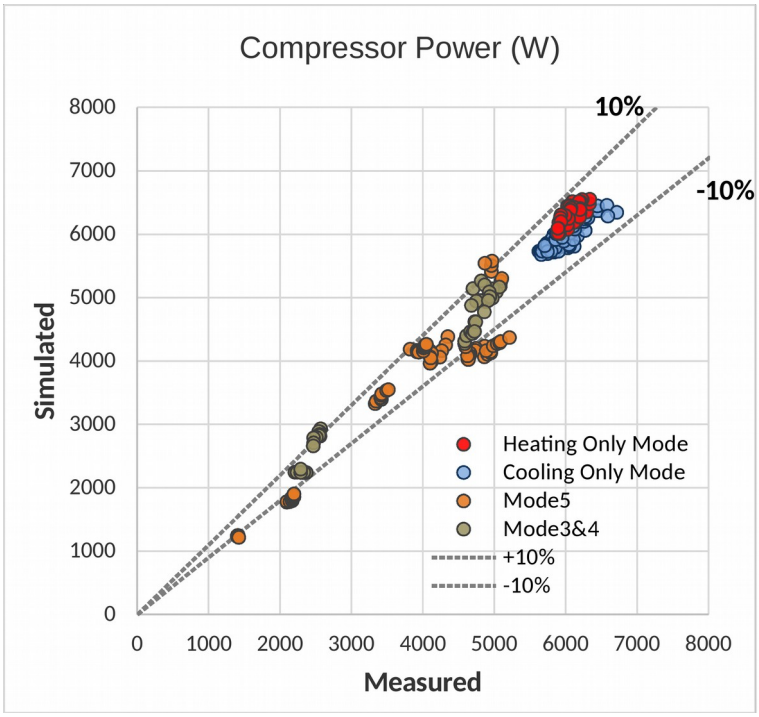

Figure 32 Comparison between the simulated and measured compressor power

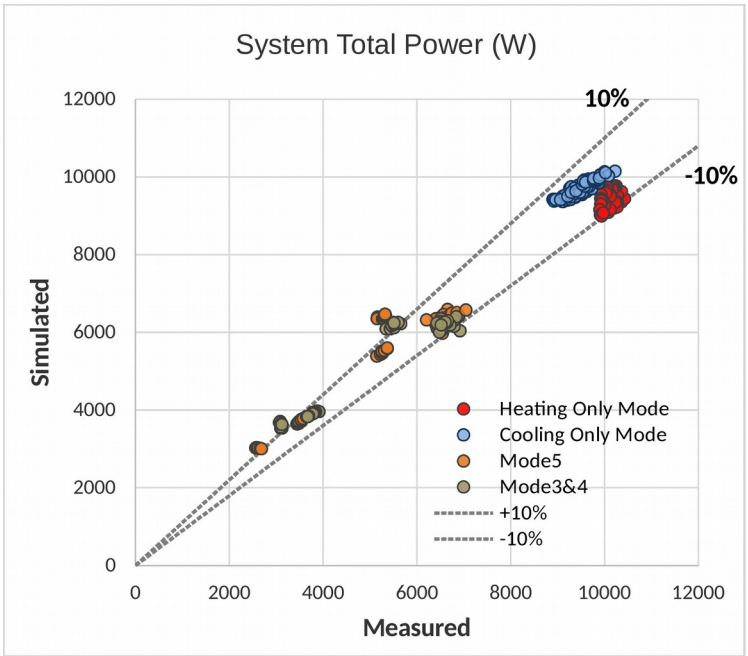

Figure 4 Comparison between the simulated and measured system total power consumption

NMBE and CVRMSE are calculated based on the simulated results and measured data, with results shown in Table 1. It can be observed that the NMBE and CVRMSE for all the modes are less than the calibration criteria, indicating the satisfactory performance of the newly developed VRF-HR model. It should also be noted that the simulated results of Mode 1 and Mode 6 are all within the ±10% range of measured data, reaffirming the accuracy of the new VRF-HP system model.

Table 1 Validation results of different operation modes and the calibration criteria

%	Calibration criteria	Mode 1	Mode 3&4	Mode 5	Mode 6
NMBE	10	2.4	2.6	2.3	-6.6
CVRMSE	30	2.8	9.5	9.6	6.9

6 Conclusions

With more adoption of VRF technologies in designing new or retrofitting existing buildings to reach the zero-net-energy goal, it is critical to have an accurate tool to assess the performance of VRF systems. This study developed a novel model to simulate the energy performance of Variable Refrigerant Flow (VRF) systems with heat recovery (HR) configurations which is capable of achieving heat recovery from cooling zones to heating zones and providing simultaneous zone cooling and heating operations. Compared with the empirical system-curve-based VRF-HR model currently implemented in several

building simulation programs, the new VRF-HR model adheres to a more physics-based development that leads to several considerable advantages in terms of modeling capability and usability. The model categorizes the operations of the VRF-HR system into six modes based on the indoor cooling/heating requirements and the outdoor unit operational states, and develops particular algorithms for each mode to address various control logics. The new model is implemented in EnergyPlus and validated with laboratory measurement data. Results show that the new model can present a satisfactory match with the measured data across all the operation modes at sub-hourly levels. The model has been adopted in the official release of the EnergyPlus simulation program since Version 8.6, which enables more accurate and robust assessments of VRF-HR system performance to support their applications in the building design and retrofitting.

Possible future works include conducting a case study and filed measurements of the actual energy performance of a real commercial building equipped with VRF-HR systems which can cover more dynamic conditions than the steady-state lab tests and thus provide further validation of the new VRF-HR model. We plan to extend the model to cover more VRF system configurations including the 2-pipe VRF and the system with water-cooled outdoor units, as well as to design a physics-based defrost cycle model by using the refrigerant parameters. In addition, we are interested to use the model to investigate the demand response capabilities of VRF by directly slowing down the outdoor unit compressors.

Acknowledgment

The authors would like to thank the Daikin U.S. Corporation and Daikin Industries LTD for the opportunity and technical support of this work. The work was also supported by the Assistant Secretary for Energy Efficiency and Renewable Energy, the U.S. Department of Energy under Contract No. DE-AC02-05CH11231.

Nomenclature

Symbols

C_{cap}	correction factor for evaporative capacity [--]
c_p	specific heat capacity of air [kJ/(kg·K)]
e_{inv}	compressor inverter efficiency [--]
D	diameter of the refrigerant main pipe [m]
f_{s_p}	functions calculating the saturated refrigerant pressure [--]
f_{s_t}	functions calculating the saturated refrigerant temperature [--]
f_{g_Cp}	functions calculating the superheating refrigerant specific heat [--]
f_{g_λ}	functions calculating the superheating refrigerant conductivity [--]

f_{g_ρ} functions calculating the superheating refrigerant density [--]

G_a volumetric flow rate of the air [m^3/s]

G mass flow rate of the refrigerant [kg/s]

H height difference between the indoor and outdoor unit nodes at the main pipe [m]

h refrigerant enthalpy [kJ/kg]

h_{fs}' enthalpy of the air leaving the outdoor unit [kJ/kg]

h_{in}' enthalpy of the air entering the outdoor unit [kJ/kg]

L refrigerant main pipe length [m]

N_{comp} electric power consumption by the compressor [kW]

N_{fan} electric power consumption by the outdoor fan [kW]

N_{out} electric power consumption by the outdoor unit [kW]

P_c condensing pressure [Pa]

P_e evaporating pressure [Pa]

P_s compressor suction pressure [Pa]

Q_{fan} sensible heat released by fan [kW]

Q_i total cooling load of the i^{th} conditioned zone [kW]

Q_{out} heat rate released from the outdoor unit [kW]

Q_{rps} evaporative capacity corresponding to rps [kW]

Q_{pipe} heat loss through the pipe [kW]

rps compressor speed [r/s]

T_c' discharge saturated temperature at the compressor outlet [°C]

T_c condensing temperature [°C]

$T_{coil,in}$ temperature of air entering the indoor coil [°C]

T_e' suction saturated temperature at the compressor inlet [°C]

T_e evaporating temperature [°C]

T_{fs} air temperature at the indoor unit coil surface [°C]

T_{out} temperature of the air leaving the indoor unit (supply air) [°C]

SC refrigerant sub-cooling degrees [°C]

SH refrigerant superheating degrees [°C]

Subscripts

$_{db}$ dry bulb temperature

$_{wb}$ wet bulb temperature

$_{rate}$ rating condition

req	required values
ref	reference condition
rps	compressor speed
PLR	partial load ratio

Appendix A: Calculation procedures for the new VRF-HR model

The algorithm of the VRF-HR Cooling Only Mode (Figure) and Heating Only Mode (Figure 6) are the same as those in the VRF-HP Cooling Mode and Heating Mode, respectively. Detailed calculation procedures for these two modes can be found in [20]. Here we only introduce the calculation procedures for the VRF-HR Simultaneous Heating and Cooling Mode.

A.1 Obtaining the building zonal load/condition information

The following building zonal load and condition information can be obtained from the zone modules within EnergyPlus:

- $Q_{in,\ total}$: zone total loads
- $Q_{in,\ sensible}$: zone sensible loads
- T_{in}: indoor air temperature
- W_{in}: indoor air humidity ratio

If there are zone cooling loads but no zone heating loads, the model goes to the VRF-HR Cooling Only Mode, the algorithms of which is the same as those for the VRF-HP Cooling Mode. If there are zone heating loads but no zone cooling loads, the model goes to the VRF-HR Heating Only Mode, the algorithms of which is the same as those for the VRF-HP Heating Mode [20]. For the rest cases, the model goes to the VRF-HR Simultaneous Heating and Cooling Mode as described below.

A.2 Calculating the I/U required evaporating and/or condensing temperature

Evaluate the required air temperature at coil surface T_{fs} and then the required evaporator refrigerant temperature $T_{e,req}$ for each indoor unit with zonal cooling requirements. Likewise, evaluate the required condenser refrigerant temperature $T_{c,req}$ for each indoor unit with zonal heating requirements. Refer to Step 1.2 in [20] for more details.

A.3 Calculating the I/U effective evaporating and/or condensing temperature

There are two refrigerant temperature control strategies for the indoor unit, i.e., *ConstantTemp* and *VariableTemp*.

- In the *ConstantTemp* strategy, *Te* and *Tc* are kept at constant values provided by the user.
- In the *VariableTemp* strategy, *Te* and *Tc* are determined using the required evaporating/condensing temperature calculated in Step 2.

A.4 Calculating the I/U condenser side piping loss

This section calculates the I/U condenser side piping loss, which occurs at the High and Low-Pressure Gas Pipe where the refrigerant flows from the O/U compressor outlets to the I/U condensers. It

includes both the refrigerant heat loss Q_{pipe} and the pressure drop ΔP_{pipe} . Note that the system performance analysis and the piping loss calculations are coupled together, because the variation of compressor operational conditions may lead to different control strategies of the system which in reverse changes the amount of piping loss. In the model, the coupling effect is addressed by numerical iterations.

At this step, the compressor discharge saturated temperature T_c' (i.e., the saturated vapor temperature corresponding to compressor discharge pressure) can be obtained using the calculated refrigerant pressure drop ΔP_{pipe} (Refer to Step 2.1 in [20] for more details).

A.5 Calculating the I/U evaporator side piping loss

This section calculates the I/U evaporator side piping loss, which occurs at Suction Gas Pipe where the refrigerant is flowing from the I/U evaporators to the O/U compressor inlets. Similar to the I/U condenser side piping loss, it includes both the refrigerant pressure drop ΔP_{pipe} and heat loss Q_{pipe}.

At this step, the compressor suction saturated temperature T_e' (i.e., saturated vapor temperature corresponding to compressor suction pressure) can be obtained using the calculated refrigerant pressure drop ΔP_{pipe}.

Note that one key input of the I/U evaporator side piping loss calculation is the enthalpy of the refrigerant at I/U evaporator inlets. It is assumed to be equal to the average enthalpy of the refrigerant at I/U condenser outlets, which is obtained in the I/U condenser side piping loss calculations (Refer to Step 2.1 in [20] for more details).

A.6 Determining the operational mode for simultaneous heating and cooling operations

As noted earlier, simultaneous heating and cooling operations include the following four modes:

- Mode 2: Cooling dominant w/o HR loss
- Mode 3: Cooling dominant w/ HR loss
- Mode 4: Heating dominant w/ HR loss
- Mode 5: Heating dominant w/o HR loss

This section describes the procedures to determine the operational mode based on the load requirements and operational conditions:

a. Calculate the required Loading Index *LI_1* satisfying the I/U cooling load (Refer to Step 2.4 in VRF-HP Cooling Mode in [20] for more details).

b. Calculate the required Loading Index *LI_2* satisfying the I/U heating load (Refer to Step 2.4 in VRF-HP Heating Mode in [20] for more details).

c. If *LI_1* <= *LI_2*, the system operates at Mode 5.

d. If *LI_1* > *LI_2* and $T_e' < T_o - T_{diff}$, the system operates at Mode 2 (T_o: outdoor air dry-bulb

temperature; T_{diff}: a constant value representing the difference between outdoor unit evaporating temperature and outdoor air temperature during simultaneous heating and cooling).

e. If *LI_1* > *LI_2* and $T_e' >= T_o - T_{diff}$, the system operates at Mode 3 or 4 (these two modes can be handled by one set of algorithms).

A.7 O/U operation analysis at Mode 5

If $T_e' < T_o - T_{diff}$, perform the following procedures:

a. Select the compressor speed corresponding to *LI_2*.

b. Calculate the compressor power corresponding to *LI_2* and the previously obtained T_c and T_e' (Refer to Step 2.6 in VRF-HP Cooling Mode in [20] for more details).

c. Calculate the evaporative capacity (*Cap_tot_evap*) provided by the compressor at *LI_2* and the previously obtained T_c and T_e' (Refer to Step 2.4 in VRF-HP Cooling Mode in [20] for more details).

d. Calculate the O/U evaporator load (*Cap_ou_evap*) based on system-level heat balance.

e. Obtain the O/U fan flow rate (*m_air_evap*) corresponding to *Cap_ou_evap*, and thus the fan power (Refer to Step 2.3 in VRF-HP Cooling Mode in [20] for more details).

If $T_e' >= T_o - T_{diff}$, perform the following procedures:

a. Select the compressor speed corresponding to *LI_1*.

b. Perform iterations between step b-i to identify the compressor Loading Index and power consumption.

c. Initialized compressor power (*Ncomp_ini*).

- For the 1st iteration step, calculate *Ncomp* = f_pow_comp(T_c, T_o – 5, *LI_2*)
- For the following iteration steps, update *Ncomp* = (*Ncomp_ini* + *Ncomp_new*)/2

d. Calculate the O/U evaporator load (*Cap_ou_evap*) based on system-level heat balance.

e. Obtain the O/U evaporating temperature T_e' level using *Cap_ou_evap* and the rated air flow rate (Refer to Step 2.3 in VRF-HP Cooling Mode in [20] for more details).

f. Update T_e level and I/U evaporator side piping loss, corresponding to T_e' update.

g. Identify the compressor Loading Index *LI_new* to provide sufficient evaporative capacity (*Cap_tot_evap*) at updated T_e' level (Refer to Step 2.4 VRF-HP Cooling Mode in in [20] for more details).

h. Calculate the compressor power (*Ncomp_new*) corresponding to *LI_new* and the updated T_e' (Refer to Step 2.6 in VRF-HP Cooling Mode in [20] for more details).

i. Compare *Ncomp_new* and *Ncomp_ini*. Start a new round of iteration if the difference is greater than the tolerance.

A.8 O/U operation analysis at Mode 2

a. Select the compressor speed corresponding to *LI_1*.

b. Calculate the compressor power corresponding to *LI_1* and the previously obtained T_c and T_e' (Refer to Step 2.6 in VRF-HP Cooling Mode in [20] for more details).

c. Calculate the evaporative capacity (*Cap_tot_evap*) provided by the compressor at *LI_1* and the previously obtained T_c and T_e' (Refer to Step 2.4 in VRF-HP Cooling Mode in [20] for more details).

d. Calculate the O/U condenser load (*Cap_ou_cond*) based on system-level heat balance.

e. Obtain the O/U fan flow rate (*m_air_cond*) corresponding to *Cap_ou_cond*, and thus the fan power.

A.9 O/U operation analysis at Mode 3 or 4

a. Select the compressor speed corresponding to *LI_1*.

b. Perform iterations between step b-e to identify the updated T_e' level within the range of T_o-5 and the original T_e'.

c. Calculate the evaporative capacity (*Cap_tot_evap*) provided by the compressor at *LI_1* and the previously obtained T_c and assumed T_e' (Refer to Step 2.4 in VRF-HP Cooling Mode in [20] for more details).

d. Calculate the O/U evaporator load (*Cap_tot_evap*) at assumed T_e' level and rated fan flow rate (Refer to Step 2.3 in VRF-HP Heating Mode in [20] for more details).

e. Perform iterations to identify the updated T_e' level to ensure the heat balance for the b. and c. calculations.

f. Update T_e level and I/U evaporator side piping loss, corresponding to T_e' update.

g. Calculate the compressor power corresponding to *LI_1* and the updated T_e' (Refer to Step 2.6 in VRF-HP Cooling Mode in [20] for more details).

h. Calculate the O/U condenser load (*Cap_ou_cond*) based on system-level heat balance.

i. Obtain the O/U fan flow rate (*m_air_cond*) corresponding to *Cap_ou_cond*, and thus the fan power.

A.10 Modifying the I/U operational parameters for capacity adjustments

The air flow rate and *SH/SC* value of each indoor unit can be controlled to adjust the cooling/heating capacity (Refer to Step 3 in VRF-HP Model in [20] for more details).

Appendix B: Example IDF snippet for a typical VRF-HR system

```
!-  ===========  OBJECTS IN CLASS: AIRCONDITIONER:VARIABLEREFRIGERANTFLOW ===========

AirConditioner:VariableRefrigerantFlow:FluidTemperatureControl:HR,
            VRF Heat Pump,   !- Name
            VRFAvailSch,     !- Availability Schedule Name
            VRFTU List,      !- Zone Terminal Unit List Name
            R410A,           !- Refrigerant Type
            autosize,        !- Rated Evaporative Capacity {W}
            0.214,           !- Rated Compressor Power Per Unit of Rated Evaporative Capacity {dimensionless}
            -6,              !- Minimum Outdoor Air Temperature in Cooling Only Mode {C}
            43,              !- Maximum Outdoor Air Temperature in Cooling Only Mode {C}
            -20,             !- Minimum Outdoor Air Temperature in Heating Only Mode {C}
            26,              !- Maximum Outdoor Air Temperature in Heating Only Mode {C}
            -20,             !- Minimum Outdoor Temperature in Heat Recovery Mode {C}
            26,              !- Maximum Outdoor Temperature in Heat Recovery Mode {C}
            VariableTemp,    !- Refrigerant Temperature Control Algorithm for Indoor Unit
            6,               !- Reference Evaporating Temperature for Indoor Unit {C}
            44,              !- Reference Condensing Temperature for Indoor Unit {C}
            5,               !- Variable Evaporating Temperature Minimum for Indoor Unit {C}
            14,              !- Variable Evaporating Temperature Maximum for Indoor Unit {C}
            36,              !- Variable Condensing Temperature Minimum for Indoor Unit {C}
            46,              !- Variable Condensing Temperature Maximum for Indoor Unit {C}
            3,               !- Outdoor Unit Evaporator Reference Superheating {deltaC}
            3,               !- Outdoor Unit Condenser Reference Subcooling {deltaC}
            0.28,            !- Outdoor Unit Evaporator Rated Bypass Factor {dimensionless}
            0.05,            !- Outdoor Unit Condenser Rated Bypass Factor {dimensionless}
            5,               !- Difference between OU Evaporating Temperature and OA Temperature in HR Mode {C}
            0.3,             !- Outdoor Unit Heat Exchanger Capacity Ratio {dimensionless}
            2.67E-2,         !- Outdoor Unit Fan Power Per Unit of Rated Evaporative Capacity {dimensionless}
            1.13E-4,         !- Outdoor Unit Fan Flow Rate Per Unit of Rated Evaporative Capacity {m3/s-W}
            OUEvapTempCur,   !- Outdoor Unit Evaporating Temperature Function of Superheating Curve Name
            OUCondTempCur,   !- Outdoor Unit Condensing Temperature Function of Subcooling Curve Name
            0.0349,          !- Diameter of Main Pipe for Suction Gas {m}
            0.0286,          !- Diameter of Main Pipe for Discharge Gas {m}
            30,              !- Length of Main Pipe Connecting Outdoor Unit to Indoor Units {m}
            36,              !- Equivalent Length of Main Pipe Connecting Outdoor Unit to Indoor Units {m}
```

```
5,                  !- Height Difference Between Outdoor Unit and Indoor Units {m}
0.02,               !- Main Pipe Insulation Thickness {m}
0.032,              !- Main Pipe Insulation Thermal Conductivity {W/m-K}
33,                 !- Crankcase Heater Power per Compressor {W}
3,                  !- Number of Compressors {dimensionless}
0.33,               !- Ratio of Compressor Size to Total Compressor Capacity {W/W}
7,                  !- Maximum Outdoor Dry-Bulb Temperature for Crankcase Heater {C}
Resistive,          !- Defrost Strategy
Timed,              !- Defrost Control
,                   !- Defrost Energy Input Ratio Modifier Function of Temperature Curve Name
,                   !- Defrost Time Period Fraction {dimensionless}
autosize,           !- Resistive Defrost Heater Capacity {W}
7,                  !- Maximum Outdoor Dry-bulb Temperature for Defrost Operation {C}
0.5,                !- Initial Heat Recovery Cooling Capacity Fraction {W/W}
0.15,               !- Heat Recovery Cooling Capacity Time Constant {hr}
1.0,                !- Initial Heat Recovery Cooling Energy Fraction {W/W}
0.15,               !- Heat Recovery Cooling Energy Time Constant {hr}
1.0,                !- Initial Heat Recovery Heating Capacity Fraction {W/W}
0.20,               !- Heat Recovery Heating Capacity Time Constant {hr}
1.0,                !- Initial Heat Recovery Heating Energy Fraction {W/W}
0.0,                !- Heat Recovery Heating Energy Time Constant {hr}
4500000,            !- Compressor maximum delta Pressure {Pa}
0.95,               !- Compressor Inverter Efficiency {dimensionless}
1,                  !- Compressor Evaporative Capacity Correction Factor {dimensionless}
3,                  !- Number of Compressor Loading Index Entries
1500,               !- Compressor Speed at Loading Index 1 {rev/min}
MinSpdCooling,      !- Loading Index 1 Evaporative Capacity Multiplier Function of Temperature Curve Name
MinSpdPower,        !- Loading Index 1 Compressor Power Multiplier Function of Temperature Curve Name
3600,               !- Compressor Speed at Loading Index 2 {rev/min}
Spd1Cooling,        !- Loading Index 2 Evaporative Capacity Multiplier Function of Temperature Curve Name
Spd1Power,          !- Loading Index 2 Compressor Power Multiplier Function of Temperature Curve Name
6000,               !- Compressor Speed at Loading Index 3 {rev/min}
Spd2Cooling,        !- Loading Index 3 Evaporative Capacity Multiplier Function of Temperature Curve Name
Spd2Power;          !- Loading Index 3 Compressor Power Multiplier Function of Temperature Curve Name
```

References

[1] DOE, Buildings Energy Data Book, Washington D.C., 2011.

[2] EPC, Directive 2010/31/EU of the European Parliament and of the Council of 19 May 2010 on the energy performance of buildings, Off. J. Eur. Union. 153 (2010) 13–35.

[3] L. Yang, H. Yan, J.C. Lam, Thermal comfort and building energy consumption implications - A review, Appl. Energy. 115 (2014) 164–173. doi:10.1016/j.apenergy.2013.10.062.

[4] L. Pérez-Lombard, J. Ortiz, C. Pout, A review on buildings energy consumption information, Energy Build. 40 (2008) 394–398. doi:10.1016/j.enbuild.2007.03.007.

[5] W. Chung, Review of building energy-use performance benchmarking methodologies, Appl. Energy. 88 (2011) 1470–1479. doi:10.1016/j.apenergy.2010.11.022.

[6] K.J. Chua, S.K. Chou, W.M. Yang, J. Yan, Achieving better energy-efficient air conditioning - A review of technologies and strategies, Appl. Energy. 104 (2013) 87–104. doi:10.1016/j.apenergy.2012.10.037.

[7] C. Sharma, R. Raustad, Compare Energy Use in Variable Refrigerant Flow Heat Pumps Field Demostration and Computer Model, ASHRAE Annu. Conf. (2013).

[8] T.N. Aynur, Variable refrigerant flow systems: A review, Energy Build. 42 (2010) 1106–1112. doi:10.1016/j.enbuild.2010.01.024.

[9] DOE, EnergyPlus Documentation Engineering Reference Version 8.6, Washington, DC, 2016.

[10] ANSI/AHRI, 2010 Standard for Performance Rating of Variable Refrigerant Flow (VRF) Multi-split Air-conditioning and Heat Pump Equipment, AHRI, Arlington, VA. (2010).

[11] B.W. Goetzler, M. Ashrae, Variable refrigerant flow systems, ASHRAE J. (2007) 24–31. doi:10.1016/j.enbuild.2010.01.024.

[12] T.N. Aynur, Y. Hwang, R. Radermacher, Simulation comparison of VAV and VRF air conditioning systems in an existing building for the cooling season, Energy Build. 41 (2009) 1143–1150. doi:10.1016/j.enbuild.2009.05.011.

[13] X. Yu, D. Yan, K. Sun, T. Hong, D. Zhu, Comparative study of the cooling energy performance of variable refrigerant flow systems and variable air volume systems in office buildings, Appl. Energy. 183 (2016) 725–736. doi:10.1016/j.apenergy.2016.09.033.

[14] D. Kim, S.J. Cox, H. Cho, P. Im, Evaluation of energy savings potential of variable refrigerant flow (VRF) from variable air volume (VAV) in the U.S. climate locations, Energy Reports. 3 (2017) 85–93. doi:10.1016/J.EGYR.2017.05.002.

[15] P. Im, J.D. Munk, Evaluation of Variable Refrigerant Flow (VRF) System Performance Using an Occupancy Simulated Research Building: Introduction and Summer Data Analysis Compared with a Baseline RTU System, in: ASHRAE Annu. Conf., 2015: pp. 1–9.

[16] L.E. Southard, X. Liu, J.D. Spitler, Performance of HVAC Systems at ASHRAE HQ: Part One, ASHRAE J. (2014).

[17] L.E. Southard, X. Liu, J.D. Spitler, Performance of HVAC Systems at ASHRAE HQ: Part Two, ASHRAE J. (2014).

[18] J.D. Spitler, L.E. Southard, X. Liu, Ground-source and air-source heat pump system performance at the ASHRAE headquarters building, in: 12th IEA Heat Pump Conf., 2017.

[19] X. Liu, T. Hong, Comparison of energy efficiency between variable refrigerant flow systems and ground source heat pump systems, Energy Build. 42 (2010) 584–589. doi:10.1016/j.enbuild.2009.10.028.

[20] T. Hong, K. Sun, R. Zhang, R. Hinokuma, S. Kasahara, Y. Yura, Development and validation of a new variable refrigerant flow system model in EnergyPlus, Energy Build. 117 (2016) 399–411. doi:10.1016/j.enbuild.2015.09.023.

[21] R. Karunakaran, S. Iniyan, R. Goic, Energy efficient fuzzy based combined variable refrigerant volume and variable air volume air conditioning system for buildings, Appl. Energy. 87 (2010) 1158–1175. doi:10.1016/j.apenergy.2009.08.013.

[22] T.N. Aynur, Y.H. Hwang, R. Radermacher, Field performance measurements of a heat pump desiccant unit in dehumidification mode, Energy Build. 40 (2008) 2141–2147. doi:10.1016/j.enbuild.2008.06.003.

[23] Y. Li, J. Wu, S. Shiochi, Modeling and energy simulation of the variable refrigerant flow air conditioning system with water-cooled condenser under cooling conditions, Energy Build. 41 (2009) 949–957. doi:10.1016/j.enbuild.2009.04.002.

[24] Y. Zhu, X. Jin, X. Fang, Z. Du, Optimal control of combined air conditioning system with variable refrigerant flow and variable air volume for energy saving, Int. J. Refrig. 42 (2014) 14–25. doi:10.1016/j.ijrefrig.2014.02.006.

[25] D. Zhao, X. Zhang, M. Zhong, Variable evaporating temperature control strategy for VRV system under part load conditions in cooling mode, Energy Build. 91 (2015) 180–186. doi:10.1016/j.enbuild.2015.01.039.

[26] T. Hong, K. Sun, R. Zhang, The New Variable Refrigerant Flow System Models in EnergyPlus : Development, Implementation and Validation, in: IBPSA Build. Simul., San Francisco, 2017.

[27] T. Hong, K. Sun, R. Zhang, O. Schetrit, R. Hinokuma, S. Kasahara, Y. Yura, Development and Validation of a New VRF Model in EnergyPlus, in: ASHRAE Winter Conf., Orlando, FL, USA, 2016.

[28] T. Hong, C. Eley, E. Kolderup, Two DOE-2 Functions Architectural Energy Corporation 142 Minna Street , San Francisco , CA 94105 , USA, in: Ninth Int. IBPSA Conf., Montreal, Canada, 2005: pp. 419–426.

[29] R. Raustad, A variable refrigerant flow heat pump computer model in energyplus, ASHRAE Trans. 119 (2013) 299–308.

[30] D.B. Crawley, L.K. Lawrie, F.C. Winkelmann, W.F. Buhl, Y.J. Huang, C.O. Pedersen, R.K. Strand, R.J. Liesen, D.E. Fisher, M.J. Witte, J. Glazer, EnergyPlus: Creating a new-generation building energy

simulation program, Energy Build. 33 (2001) 319–331. doi:10.1016/S0378-7788(00)00114-6.

[31] ANSI/ASHRAE, ASHRAE Guideline 14-2014 Measurement of Energy and Demand Savings, ASHRAE. (2014).